

## PIC simulations of relativistic electron flows: The fastest-growing mixed mode and the electromagnetic finite grid instability

M.E. Dieckmann<sup>1</sup>, J.T. Frederiksen<sup>2</sup>, A. Bret<sup>3</sup>, P.K. Shukla<sup>1</sup>

<sup>1</sup> Faculty of Physics & Astronomy, 44780 Bochum, Germany

<sup>2</sup> Stockholm Observatory, 10691 Stockholm, Sweden

<sup>3</sup> ETSI Ind., University of Castilla La Mancha, 13071 Ciudad Real, Spain

### Abstract

Instabilities driven by two electron beams that stream at the relativistic relative velocity  $\mathbf{v}_b$  are important as a plasma thermalization and magnetic field generation mechanism in astrophysics [1, 2] and in inertial confinement fusion [3]. The time-evolution of such instabilities, which are subdivided into the two-stream, mixed mode and filamentation (beam-Weibel) instability [4], is multi-dimensional and nonlinear and the instabilities are usually modelled with particle-in-cell (PIC) simulations. We examine the wave spectrum we obtain, if both beams have a density ratio 9 and  $(1 - v_b^2/c^2)^{-1/2} \approx 4$ . The mixed mode dominates and grows fastest for highly relativistic  $|\mathbf{v}_b|$ . An electromagnetic finite grid instability is shown to generate artificial magnetic fields, imposing a simulation constraint [5].

### Particle in cell (PIC) simulation

PIC codes solve the Maxwell's equations and the relativistic Lorentz equation for computational particles, each with index  $i$ , charge  $q_c$  and mass  $m_c$  according to

$$\nabla \times \mathbf{B} = \mu_0 \mathbf{j} + \epsilon_0 \mu_0 \frac{\partial \mathbf{E}}{\partial t}, \quad (1)$$

$$\nabla \times \mathbf{E} = -\frac{\partial \mathbf{B}}{\partial t}, \quad (2)$$

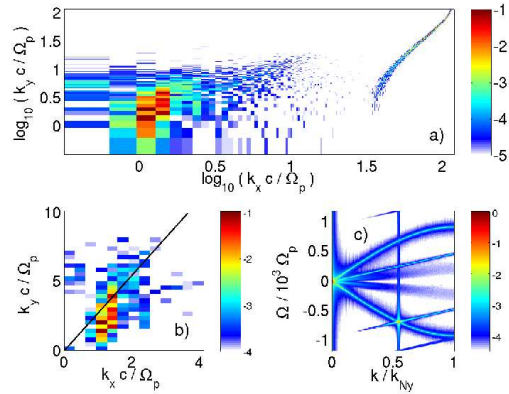


Figure 1: Panels (a,b) show the 10-logarithmic power spectrum of  $E_x(x,y) + iE_y(x,y)$  in the 2D simulation at  $t_0\Omega_p = 35$ . Panel (b) displays the low  $\mathbf{k}$  branch formed by the two-stream ( $k_y = 0$ ) and the mixed modes ( $k_y \neq 0$ ) with  $k_x \approx \Omega_p/c$ . A line cuts (b) at  $\alpha_M = 72.5^\circ$ . Panel (c) illustrates the electromagnetic power spectrum (dispersion relation) along this direction in the 1D simulation with  $\alpha = \alpha_M$  integrated over  $0 < t\Omega_p < 1.9$ .

$$\frac{d\mathbf{p}_i}{dt} = q_c(\mathbf{E} + \mathbf{v}_i \times \mathbf{B}), \quad \frac{d\mathbf{x}_i}{dt} = \mathbf{v}_i. \quad (3)$$

The particles and fields interact through the current  $\mathbf{j}$ . The vacuum permittivity and permeability are  $\epsilon_0$  and  $\mu_0$  and the momentum is  $\mathbf{p}_i = m_c \Gamma_i \mathbf{v}_i$ . We consider computational electrons with a physical charge-to-mass ratio  $q_c/m_c = -e/m_e$ . Our simulation scheme [6] fulfils  $\nabla \cdot \mathbf{E} = \rho/\epsilon_0$  and  $\nabla \cdot \mathbf{B} = 0$  to round-off precision.

Two beams are modelled, each consisting of equal numbers of electrons and protons with the masses  $m_p = 1836 m_e$ . The proton dynamics is neglected. The thermal speeds of both electron beams  $v_e = (K_B T_e / m_e)^{1/2} = c/10$ . The plasma frequencies of the bulk (beam) electrons is  $\omega_1 = 10^5 2\pi/s$  ( $\omega_2 = \omega_1/3$ ). The total plasma frequency is  $\Omega_p = \sqrt{\omega_1^2 + \omega_2^2}$ .

The electron skin depth is  $\lambda_e = v_e/\Omega_p$ . A 1D simulation resolves the length  $L_1 = 72.5\lambda_e$  with 33000 cells. A 2D simulation resolves a plane  $20\lambda_e \times 20\lambda_e$  by  $750 \times 750$  grid cells. The boundary conditions are periodic and the simulation box is the rest frame of the bulk electrons. The beam electrons move at the mean speed  $|v_b|$  with  $\Gamma(v_b) = 4.09$ . The beam moves along the x-direction in the 2D simulation. The one-dimensional simulation box is oriented at the angle  $\alpha_M = 72.5^\circ$  relative to  $\mathbf{v}_b$  and also at the angles  $\alpha = 0^\circ$  and  $\alpha = 90^\circ$ .

## Simulation results

The electron beams result in unstable wavevectors  $\mathbf{k}$  that form with  $\mathbf{v}_b$  a broad range of angles  $\alpha$  [4]. The growth rate is a function of  $\alpha$  and it is  $\sim \Gamma^{-1}$  for the two-stream instability ( $\alpha = 0$ ), it is  $\sim \Gamma^{-1/2}$  for the filamentation instability ( $\alpha = 90^\circ$ ) and it is  $\sim \Gamma^{-1/3}$  for the fastest-growing mixed mode ( $\alpha = \alpha_M$ ).

Figures 1(a,b) display the power spectra of the electric field at its saturation time  $t_0$  in the 2D simulation plane. Branches exist in (a) at low  $|\mathbf{k}|$  and at large  $|\mathbf{k}|$ . The filamentation branch ( $k_x = 0$ ) is weak. The wave branch in the 2D simulation at low  $|\mathbf{k}|$  is due to the (physical) electron beam driven instability [4], while the high  $|\mathbf{k}|$  branch is a numerical sideband instability that gives rise to an artificial magnetic field growth, as Fig. 1(c) displays [5]. The

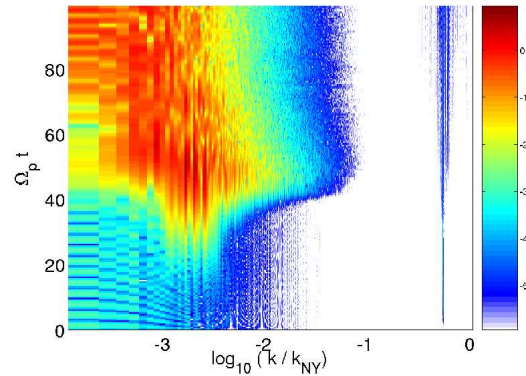


Figure 2: The power spectrum of the box-aligned electric field component in the 1D simulation: The fastest-growing mixed mode instability grows and saturates at low  $k$ , while the numerical instability develops at high  $k$ .

maximum wavenumber resolved by the 1D simulation with its cell size  $\Delta_x$  is  $k_{Ny} = \pi/\Delta_x$ . The high- $k$  branch in (a) and (c) is a sideband of the beam mode  $\Omega \approx kc \cos(\alpha_M)$  in the 1D simulation. The sideband is separated by  $\Delta\Omega = 2\pi/\Delta_t = 10^3\Omega_p$ , where  $\Delta_t = \Delta_x/v_b$ .

The simultaneous and initially independent growth of the physical and the numerical instabilities is exhibited by Fig. 2, which shows the time evolution of the  $k$ -power spectrum in the 1D simulation with  $\alpha = \alpha_M$ . A broadening of the high- $k$  instability takes place when the low- $k$  instability saturates at  $t\Omega_p \approx 40$ , presumably due to the spread in the electron velocities and thus in the time during which beam electrons cross one simulation cell.

The importance of the finite grid instability is determined in Ref. [5] by comparing the time-evolution of the electron kinetic energy- and electric field energy densities in the 1D simulation with their counterparts in the 2D simulation. After its saturation, the energy density of the (physical) mixed mode in the 1D simulation is comparable to that of the artificial sideband mode in the 2D simulation. The finite grid instability, which is a consequence of the PIC approximation and could be detected with two different PIC codes [5], thus leads to a significant growth of artificial electromagnetic fields in multi-dimensional PIC simulations.

The 1D simulation allows us to pick specific angles  $\alpha$  between the  $\mathbf{k}$ -vectors of the waves and  $\mathbf{v}_b$ , while the finite grid instability is weak due to the high spatial resolution. We can compare the growth of the two-stream modes  $\alpha = 0$  and the filamentation modes  $\alpha = 90^\circ$  with that of the mixed modes. We select the fastest-growing mixed mode with  $\alpha = \alpha_M$  [4]. We keep the plasma parameters unchanged except for  $\Gamma$ , which we take to be 4, 16 and 256. This band covers the typical speeds of accretion disc jets [1, 2]. Figure 3 shows the box-averaged energy densities  $\epsilon_0\mathbf{E}_X^2$  of the electric field parallel to the 1D simulation direction  $X$ . The two-stream instability always grows slowest, while the mixed mode grows fastest. The filamentation mode has an intermediate growth rate.

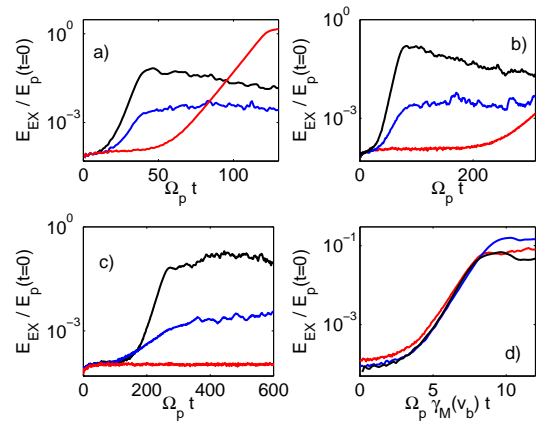


Figure 3: The box-averaged, box-aligned electric field energy densities: (a) is  $\Gamma = 4$ , (b) is  $\Gamma = 16$  and (c) is  $\Gamma = 256$ . Red: two-stream instability, black: mixed mode instability and blue: filamentation instability. Panel (d) compares the electric field energy densities produced by the mixed modes in the three 1D simulations. The time axis in (d) is multiplied with the linear growth rates  $\gamma_M \sim \Gamma^{-1/3}$  of the respective mixed modes. The curve for  $\Gamma = 4$  (black),  $\Gamma = 16$  (blue) and  $\Gamma = 256$  (red) overlap, confirming the  $\gamma_M$  scaling.

## Summary

- Particle-in-cell simulation codes are a standard method to examine particle acceleration and magnetic field generation in astrophysical plasma. However, for relativistic plasma flow speeds the well-known finite grid instability develops a strong electromagnetic component: This instability results in the growth of strong unphysical magnetic fields, while the total simulation energy is approximately constant. Typically, numerical instabilities are associated with an exponentially growing total simulation energy.
- For relativistically colliding plasma the mixed mode instability outgrows the filamentation (beam-Weibel) instability, unless the densities of the colliding plasmas are similar [7]. Previously only filamentation modes have been discussed in this context. The nonlinear saturation is thus due to flux tube formation and particle phase space hole formation [5].

## Acknowledgements

The authors thank the German Research Foundation (DFG) for financial support and the Swedish high-performance computer center north (HPC2N) for computer time and support.

## References

- [1] T. Piran, Rev. Mod. Phys. **76** 1143 (2004)
- [2] J.C.A. Miller-Jones, R.P. Fender, E. Nakar, Mon. Not. R. Astron. Soc. **367** 1432 (2006)
- [3] R.J. Mason, M. Tabak, Phys. Rev. Lett. **80** 524 (1998)
- [4] A. Bret, M.C. Firpo, C. Deutsch, Phys. Rev. Lett. **94** 115002 (2005)
- [5] M.E. Dieckmann, J.T. Frederiksen, A. Bret, P.K. Shukla, Phys. Plasmas **13** 112110 (2006)
- [6] J.W. Eastwood, Comput. Phys. Comm. **64** 252 (1991)
- [7] A. Bret, L. Gremillet, J.C. Bellido, Phys. Plasmas **14** 032103 (2007)